

A DETAILED VIEW ON THE MIXING AND LOSS GENERATION PROCESS DURING STEAM ADMISSION CONCERNING GEOMETRY, TEMPERATURE AND PRESSURE

D. Engelmann – R. Mailach

Ruhr-Universität Bochum, Chair of Thermal Turbomachinery, 44780, Bochum, Germany,
David.Engelmann@rub.de

ABSTRACT

Steam turbines used in industrial applications often contain several branches for the admission of steam. Those branches are placed at the axial connections of two stage groups or within a single module. Among geometrical parameters, different temperature and pressure levels have a great impact on the mixing process of main and branch mass flows and on the flow distribution in subsequent turbine stages. Therefore, it is essential to understand the loss mechanisms appearing at junctions of different mass flow partitions to guarantee a stable operation and a high efficiency in a wide range of steam load.

A comprehensive parameterized numerical study of a generic steam admission junction is described in this paper which focusses on geometry dependencies as well as on temperature and pressure differences. The study is performed with a 3D RANS solver to determine several loss partitions, such as total pressure loss, wall friction and admission loss. The results of the flow simulations are compared to literature values and empirical loss assumptions with a detailed view on both main steam path and branch pipe.

NOMENCLATURE

A	m ²	area	Subscripts	
a	m	width of main channel	adm	admission
AR	%	area ratio, b/a	CS	cross sectional
b	m	width of branch channel	fr	friction
FR	%	flow ratio, $\dot{m}_{Br}/\dot{m}_{Out}$	In	inlet
\dot{m}	kg/s	mass flow	Out	outlet
P	m	Perimeter	Br	branch
p	Pa	pressure	Sf	surface
T	°C	temperature	t	total
TR	%	transition radius related to outlet diameter	W	wall
Greek Symbols			Abbreviations	
ζ	-	pressure loss coefficient	K	kink
τ_w	N/m ²	wall shear stress	v	vapour
			w	water

INTRODUCTION

Modern steam turbines are not only used for electric power generation in fossil power plants but rather satisfy a wide range of industrial applications. They can be found in the process of Fluid Catalytic Cracking (FCC) or Carbon Dioxide Capture and Storage (CCS). They are furthermore utilized in captive power plants e.g. for paper mills, mining, food production, the chemical industry

or applied in Concentrated Solar Power plants (CSP) and within Combined Heat and Power (CHP). This huge field of applications with its diverse demands requires a flexible, modular and compact design of industrial steam turbines. Therefore, the control stage as well as several interchangeable high, intermediate and low pressure modules are combined together within a single turbine casing. In contrast to common power plant turbines, they feature a high and also variable rotational speed up to 18,000 RPM with an output range of a few kilowatt to a maximum value of today 200 MW.

Usually, an industrial steam turbine includes several branches which are placed at the axial connections of two stage groups or within a single module. Steam admission through these branches can have a serious impact on the operational behaviour of a steam turbine. When the branch mass flow joins the main steam path flow an additional secondary pressure loss occurs which is caused by the deflection and the inhomogeneous mixing process of the admitted steam with main flow partitions. The amount of loss depends on rotational speed, junction geometry and steam parameters such as degree of admission, pressure level and temperature. Therefore, it is important to estimate the loss mechanisms appearing at these junctions to enable a high efficiency together with a stable operation despite the variation in the steam load.

In literature several loss mechanisms are described for the main flow path of gas and steam turbines with shrouded blades. Denton (1993) e.g. provided formulations for the estimation of losses which are caused by the interaction of the re-entering shroud cavity flow with the blade channel flow. Some more loss mechanisms are given by Wallis et al. (2000) which studied turning device configurations in order to reduce shroud cavity losses in a four stage axial turbine. They reported four types of losses concerning labyrinth seals, counter rotating cavity walls, flow mixing at the cavity outlet and subsequent stages. Gier et al. (2003) applied these given loss definitions to a numerical investigation of a three stage low pressure turbine for jet engines and added another loss mechanism which is caused by steps at the sidewalls of the flow path.

A lack of information exists regarding the influence of turning, mixing and separation of branch mass flow partitions and its related additional secondary pressure loss or in other words admission loss. The reason behind this are missing experimental results, which are connected one the one side with a compact steam turbines design and on the other side with adverse fluid conditions. Thick-walled, pressure-stable casings and guide vane carriers hamper the local accessibility for measurement probes or optical systems. Moreover, water-vapour raises the demands for measurement equipment. Condensate can block sensor heads or wall pressure taps and thereby falsify the experimental output.

By now, the most convenient data in the open literature is given by Idelchik (1986) and Miller (1990). They collected pressure loss data for fluid flow through pipes and specific components such as sudden openings, valves, manifolds, nozzles and flow junctions while some new attempts deal with the estimation of pressure losses for turbine blade coolant flows. Barringer et al. (2014) for example provide numerical and experimental data for static pressure losses of inlet and exit holes in a generic up-scaled coolant channel with air at ambient conditions.

Numerical studies for T-junctions with circular pipes were performed by Walker et al. (2010). They adjusted the parameters of several common RANS turbulence models to improve the prediction of the downstream flow mixing. Kuczay et al. (2010), on the other hand, used LES simulations to gain more insights of the thermal mixing downstream the junction. Both publications relate to experiments of Andersson et al. (2006) who investigated the flow mixing in a pipe-junction with a temperature difference of 15 K between inlet and branch pipe. However, all mentioned sources neither directly refer to admission in steam turbines nor use vapour as fluid in combination with a high pressure and temperature level. Likewise, prediction of admission in steam turbines is sophisticated due to asymmetrical inflow and inhomogeneous flow mixing which cause a complex 3D flow field and concomitant a high numerical effort.

With the aim to gain more information about admission losses in industrial steam turbines several numerical studies with a generic T-junction were performed in the recent past. Therefore, in the first part of this publication a brief summary of past research activities is given. This concerns

geometry details, loss calculation method, fluid parameters as well as achieved results which are partially already published. Whilst the past investigations solely focus on loss values for the main steam path, a detailed view on both main steam path and branch pipe is given here. The second part deals with temperature and pressure differences at the inlet of main path and branch pipe and their effects on the mixing and loss generation process.

T-JUNCTION GEOMETRY AND SIMULATION PROCEDURE

Several issues arise if one attempt to use admission loss values from the literature for steam turbines. Experimental data given by Idelchik (1986) and Miller (1990) are based on flow through pipe junctions with water at ambient condition (see Figure 1, left).

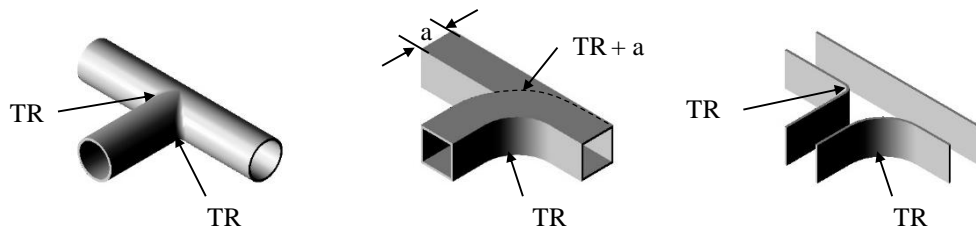


Figure 1: Comparison of pipe junctions with rounded transitions; Left: circular pipe junction (Miller (1990)); Middle: rectangular pipe junction with beneficial flow guide (Idelchik (1986)); Right: generic T-junction for parameterized numerical study

However, in a typical industrial steam turbine vapour at high temperature and pressure is admitted through semi-detached branches or through circumferential slots. Two examples of such industrial steam turbines are given in Figure 2 and studied by Engelmann et al. (2012, 2013 and 2014). The left sketch shows a typical admission turbine with high mass flow proportions through the branches which induces a distortion in the flow field over the circumference. The right drawing by contrast describes a turbine segment with a circumferential slot. Mass flow used for axial thrust balancing at the balance piston is guided back the main steam path through this slot.

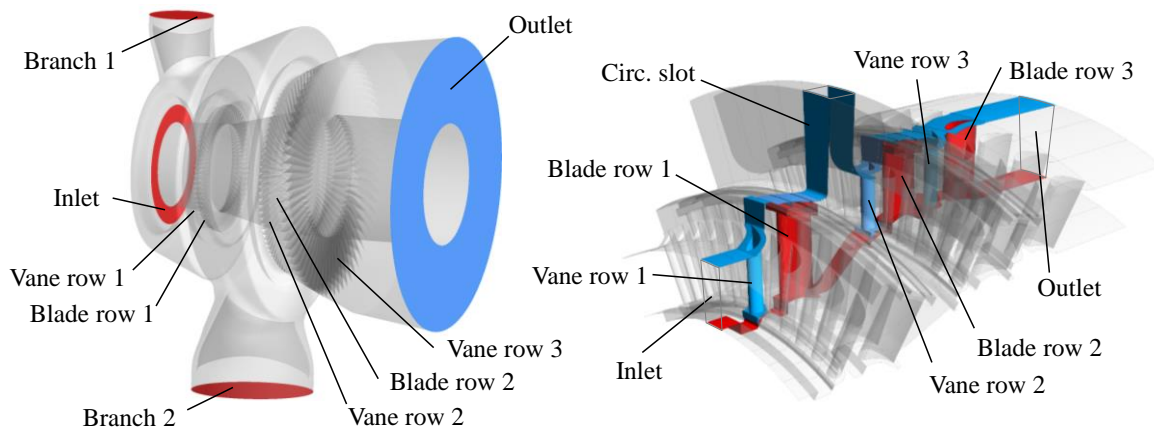


Figure 2: Examples of industrial steam turbines; left: 2.5-stage section with two semi-detached branches; right: 3-stage configuration with a circumferential slot for steam admission

Thus, on the one side a geometry is needed which mirrors primary inflow and deflection behavior of both pipe junction and steam turbine. On the other side a parameterizable topology is required in order to reveal as many influence factors as possible together with a moderate numerical effort. Therefore, a generic 2-dimensional T-junction with translational periodic boundaries instead of sidewalls is chosen which feature radial inflow and a 90 degree deflection related to the main flow path (see Figure 1, right). With that shape it is possible to combine mesh generation, simulation and loss evaluation within an automated numerical procedure. This also enables the

calculation of loss values for a huge combination of mass flows, area ratios, and transition radii as well as for several turbulence models and fluid properties.

An overview of major geometric parameters of the T-junction is given in the schematic drawings of Figure 3. There, distance a is the hydraulic diameter respectively width of the main flow path and reference for all other length and area values. Width b represents the diameter of the branch and is calculated in dependency of the actual area ratio AR and distance a . All other geometry details such as channel length and transition radii are generated as a function of a and b . According to literature each flow section is 70-times longer than distance a . This supports a full developed velocity profile for inlet and bleed region. Furthermore, fluctuations and flow separations caused by deflection are able to decay before reaching the outlet of the numerical domain.

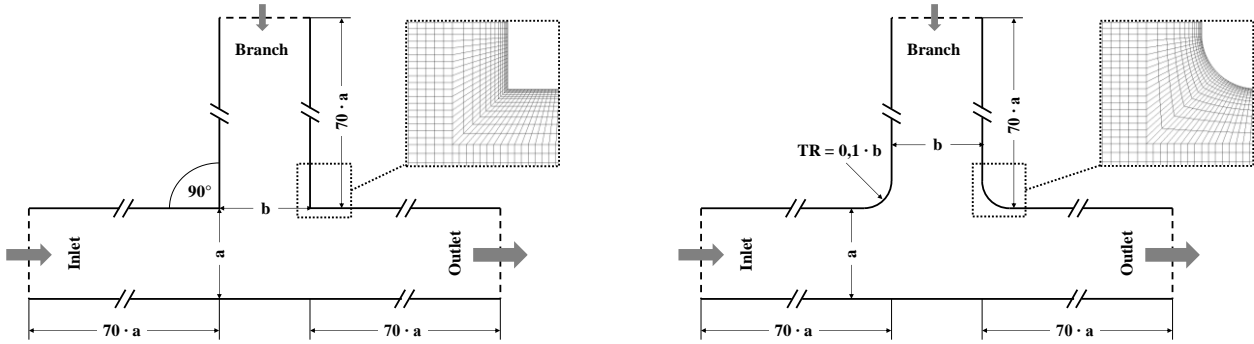


Figure 3: Geometric parameters for the T-junction (left: sharp transitions; right: rounded transitions) with details of the numerical mesh

The automated numerical study is realized by the usage of a PERL routine with integration of the commercial mesh creator ICEM CFD and the numerical solver ANSYS CFX via scripts and sub-routines. As described by Engelmann et al. (2012), a block structured hexahedron mesh is used which consists of in total 64,000 elements and includes mesh refinements towards the walls and at the junction zone. All simulations are performed with the $k-\omega$ based SST turbulence model including a so called reattachment modification (SST-RM) for better prediction of flow separation and reattachment at walls. In a prior publication (Engelmann et al. (2013)) the almost negligible influence of common turbulence models is discussed together with the effect of varying fluid properties (water, air, overheated steam) on the loss distribution. But here only two fluids are regarded. Namely, on the one side water with a constant density for the comparison with the given literature data and on the other side vapour as compressive single-phase real gas in accordance with the international properties steam table IAPWS-IF97 which is more convenient for the transferability to steam turbines. Nevertheless, over 800 predictions are performed for the current study. Some more details concerning the PERL routine and simulation procedure are given by Engelmann et al. (2013).

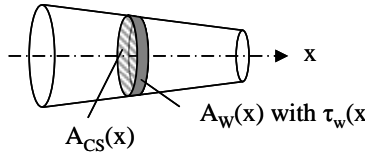
LOSS CALCULATION METHOD

Literature admission loss data from Idelchik (1986) and Miller (1990) are described in terms of a total pressure loss coefficient with exclusion of pipe friction loss. Therefore, to compare gained numerical values with experimental data from the literature sources it is necessary to explain the used loss calculation method and how the several loss partitions are specified.

First of all, the total pressure loss coefficient ζ_t for the main flow path is calculated with mass flow averaged values of total pressure for inlet and outlet which are related to the dynamic pressure at the outlet (see equation (1)).

$$\zeta_t = \frac{p_{t,In} - p_{t,Out}}{p_{t,Out} - p_{Out}} \quad \zeta_{fr} = \frac{\Delta p_{fr}}{p_{t,Out} - p_{Out}} \quad \zeta_{adm} = \zeta_t - \zeta_{fr} \quad (1)$$

Total pressure loss contains friction loss as well as admission loss caused by flow deflection, separation, vortex shedding and mixing of concerned flow partitions. Therefore, the friction loss coefficient ζ_{fr} which depends on the pressure loss Δp_{fr} and is induced by wall friction is considered next. Usually, the amount of friction is determined as a function of pipe diameter, pipe length and a friction factor based on empirical formulations from Nikuradse, Blasius and Colebrook using the local Reynolds number and wall roughness (see Schlichting and Gersten (2006)). This works pretty good for simple geometries such as pipes with constant diameter. But with regard to steam turbines and their complex geometries another approach is chosen which is given in equation (2). It is based on descriptions from Schlichting and Gersten (2006) and uses local wall shear stress $\tau_w(x)$, wall surface $A_w(x)$ and perpendicular cross sectional area $A_{CS}(x)$. The x -coordinate in equation (2) indicates the position on the meridian streamline while $P(x)$ is the perimeter of the corresponding local flow path.

$$dp_{fr} = \frac{\tau_w(x) \cdot P(x)}{A_{CS}(x)} dx \quad \text{with} \quad A_w(x) = P(x) \cdot dx \quad (2)$$


Integration of the partial friction loss dp_{fr} along the meridian stream line leads to the friction loss Δp_{fr} of the actual flow path (see equation (3), left term). Since CFD solvers use finite volumes, it is possible to calculate the pressure loss Δp_{fr} by using the product of local wall shear stress $\tau_w(x)$ and its corresponding finite wall element related to the local cross sectional area. Subsequently, summing up this product over the surface of the regarded flow path from inlet to outlet leads to $\Delta p_{fr,CFD}$ (see equation 3, right term). As one can assume, friction loss accuracy is directly connected to the grid density, thus to the size of the wall elements.

$$\text{Analytical: } \Delta p_{fr} = \int \frac{\tau_w(x) \cdot P(x)}{A_{CS}(x)} dx \quad \text{CFD: } \Delta p_{fr,CFD} = \sum_{i=1}^n \frac{\tau_w(x_i) \cdot A_w(x_i)}{A_{CS}(x_i)} \quad (3)$$

At last, the admission loss coefficient ζ_{adm} can be derived when subtracting ζ_{fr} from ζ_t (see equation (1)). All equations explained in the last passage are valid for the branch pipe if $p_{t,In}$ is replaced with $p_{t,Br}$. The admission loss coefficient ζ_{adm} is equal to the total pressure loss coefficient given in literature and therefore used to validate the numerical results of the T-junction study against literature values.

NUMERICAL RESULTS

Loss coefficients of the T-junction compared to literature values

The diagrams in Figure 4 and Figure 5 show the distribution of total, friction and admission loss coefficients as function of the flow ratio FR for the open accounting from inlet to outlet (left diagrams) and from branch to outlet (right diagrams). Results for both sharp and rounded transitions are compared to literature values, whereby for rounded transition the T-junction with a transition ratio of 10% is chosen for comparison in accordance with literature data (see Figure 5). The numerical results are based on predictions with water as fluid at a temperature of 25°C to ensure comparability with literature data. An average static pressure of 10^5 Pa is set at the outlet pipe boundary. Specific mass flow values are defined at inlet and branch boundary to gain an overall Reynolds number of $2.15 \cdot 10^5$. All predictions are performed with an increment of 5 % for the flow ratio FR to generate the loss curves.

Regardless whether the amount of friction is determined as function of wall shear stress or with the usage of empirical formulations a nearly equivalent progression of the loss coefficients is

gained. Moreover, an overall good agreement with the experimental values is reached for the admission loss coefficient even though there is a discrepancy between the losses given by Idelchik (1986) and the ones given by Miller (1990). In the case of sharp transitions both authors consider the same pipe topology but describe different loss curves, especially for ζ_{Br-Out} (see Figure 4, right diagram). In the case of rounded transitions Miller (1990) provides results for pipes with circular cross sectional areas. However, Idelchik (1986) solely states data for a pipe junction with rectangular cross sectional area but beneficial flow guidance (compare Figure 1, middle). This explains the spread of the specific admission loss coefficient curves.

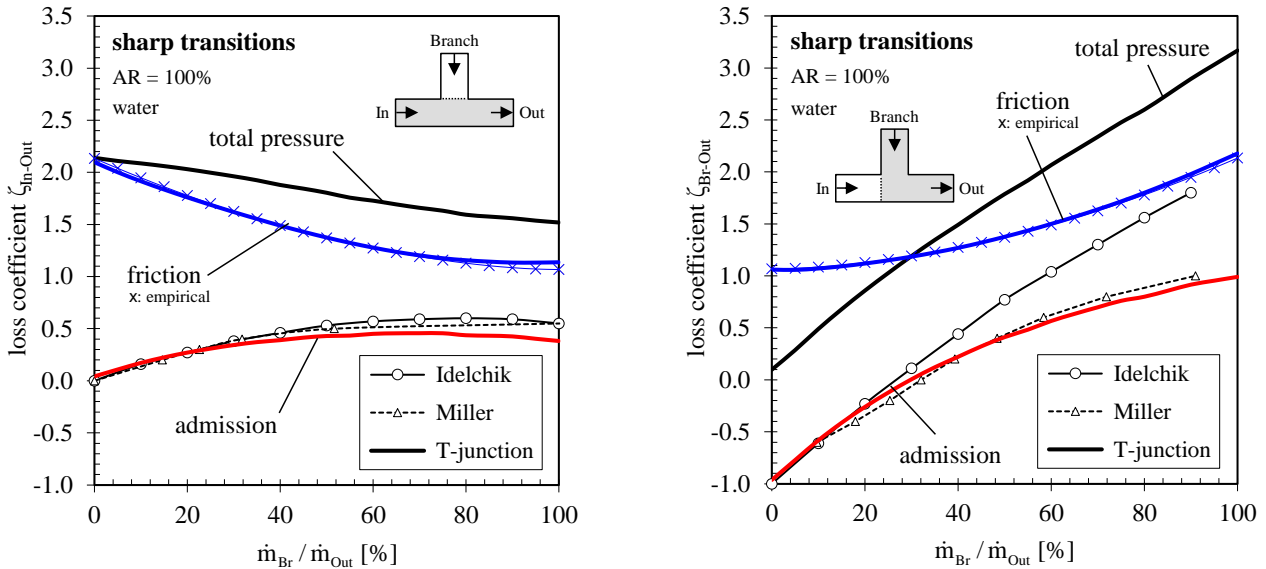


Figure 4: Distribution of total, friction and admission loss coefficient ζ_{In-Out} and ζ_{Br-Out} for the T-junction with sharp transitions compared to literature values, AR = 100%

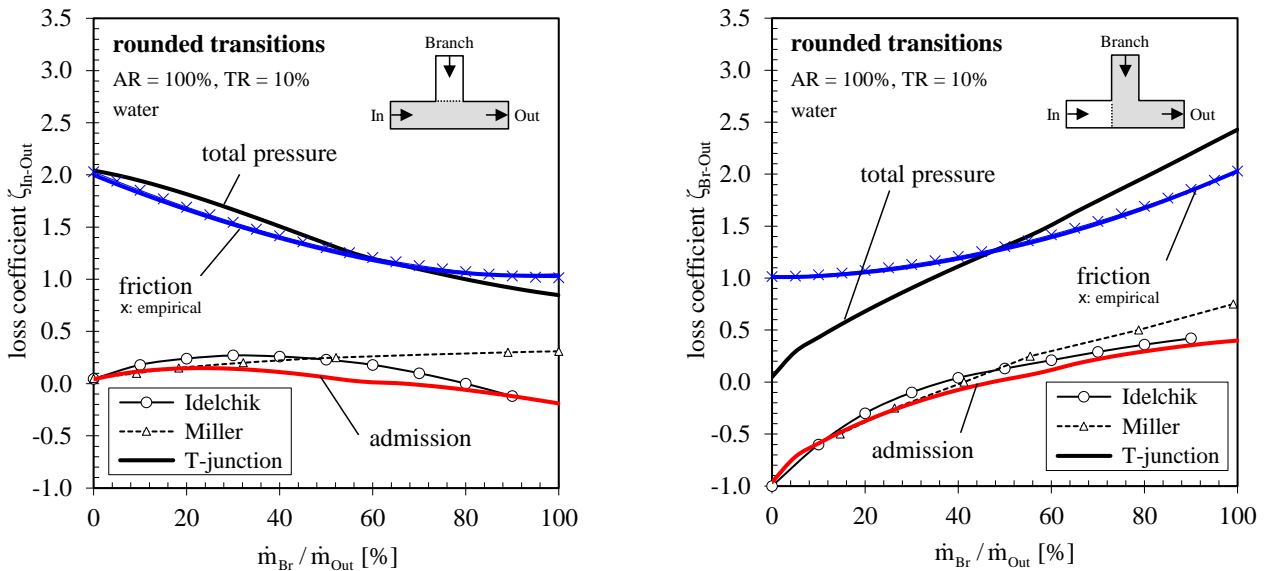


Figure 5: Distribution of total, friction and admission loss coefficient ζ_{In-Out} and ζ_{Br-Out} for the T-junction with rounded transitions compared to literature values, AR = 100%, TR = 10%

But there are some more characteristics and minor differences in the specific admission loss curves. First of all a negative loss value can occur which is ascribable to the open accounting from e.g. inlet to outlet without regarding the branch boundary and vice versa. The negative admission loss becomes conspicuous if the accounting is done from branch to outlet (see Figure 4 and

Figure 5, right diagrams). For a zero flow ratio FR the whole mass flow is contributed by the inlet channel. In this case, total and static pressure in the branch channel as well as static pressure within the junction zone show almost the same values. Due to the inlet mass flow with its high velocity, total pressure is higher than static pressure within the junction zone. This leads to a rapid rise of the branch total pressure when reaching the junction zone which then in turn is decreased in the outlet channel mainly because of the friction loss. As the curves in the right diagrams of Figure 4 and Figure 5 illustrate, there is only a small $\Delta p_{t, Br-Out}$ and therefore $\zeta_{t, Br-Out}$. As opposed to this, $\Delta p_{fr, Br-Out}$ and therefore $\zeta_{fr, Br-Out}$ are much higher because they are mainly driven by the high velocity of the inlet mass flow.

When looking at ζ_{In-Out} , there is a small but already existing amount of admission loss for a flow ratio $FR = 0\%$. The reason for this can be found in fluid partitions coming from the inlet channel which enter and circulate inside the branch channel when crossing it. Unfortunately, this effect is not considered in the literature for the accounting from inlet to outlet (see Figure 5, left). Furthermore, increasing the branch flow leads to a minor under-prediction of the numerical loss coefficients. This effect is attributable to the absence of sidewalls for the T-junction (see Figure 1). Similar to the flow behaviour in a 90° -manifold and due to deflection of the branch flow a pressure gradient between inner and outer bend arises. As a result of side wall friction in pipe junctions with circular or rectangular cross sectional area, a cross flow perpendicular to the main flow is formed to counterbalance this pressure gradient. Interaction of the cross flow with the main flow then leads to a higher secondary loss coefficient. In contrast to this, the pipes of the flat T-junction do not have sidewalls which means a comparable cross flow does not arise. Finally, rounded transitions lead to reduced admission loss values compared to sharp transitions. This can be explained with better flow guidance, a later separation of the deflected branch flow (compare the several kinks K1 to K4 in Figure 6 and Figure 7) and a smaller separation zone as mentioned by Engelmann et al. (2014).

Geometrical influences

Due to clarity reasons, the loss curves in the diagrams above are plotted for only one specific geometry. Therefore, in this chapter the influence of the area ratio AR and the transition radius TR on the admission loss is discussed.

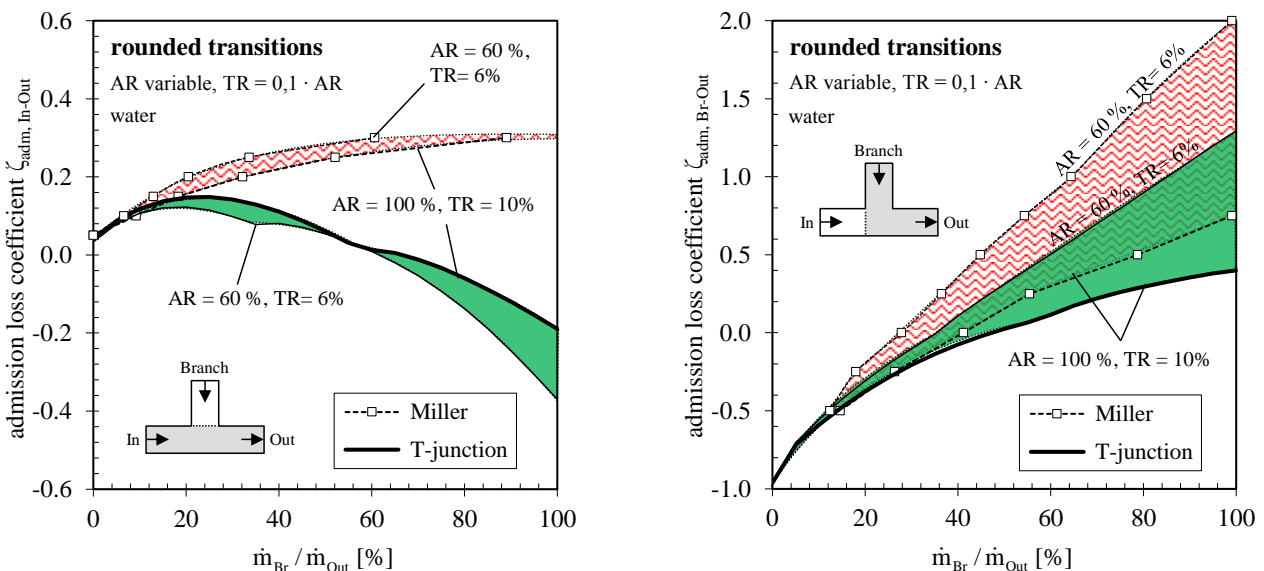


Figure 6: Combined geometrical influence on the admission loss coefficient $\zeta_{adm, In-Out}$ and $\zeta_{adm, Br-Out}$ for the T-junction with rounded transitions when TR is a function of AR

Again, there is a discrepancy between measurement data given by Miller (1990) and Idelchik (1986). Idelchik provides only one loss curve being representative for all area ratios

whereas Miller describes a small spread in the loss curves (Figure 6, left) for the accounting domain from inlet to outlet. In contrast to this, Idelchik describes several curves apparently without uniform classification and together with a wide value spread whereas Miller provides a systematic spread (Figure 6, right) for the accounting from branch to outlet. As a consequence, the loss data from Idelchik is omitted in the following diagrams since the geometric topology of T-junction and Millers pipe junction is similar and therefore more convenient for the comparison of loss values.

Figure 6 shows the effect on the admission loss in form of a combined geometry modification. In other words TR is defined as a function of AR which in turn is a function of the branch channel width b . In the left diagram of Figure 6 a maximum spread $\Delta\zeta_{adm, In-Out}$ of 0.29 for the numerical loss values at maximum flow ratio FR is recognisable whereas the right diagrams shows a maximum spread $\Delta\zeta_{adm, Br-Out}$ of 1.35. This difference can be explained if the governing geometric parameters TR and AR are separately considered and varied starting with the base values $TR = 10\%$ and $AR = 100\%$.

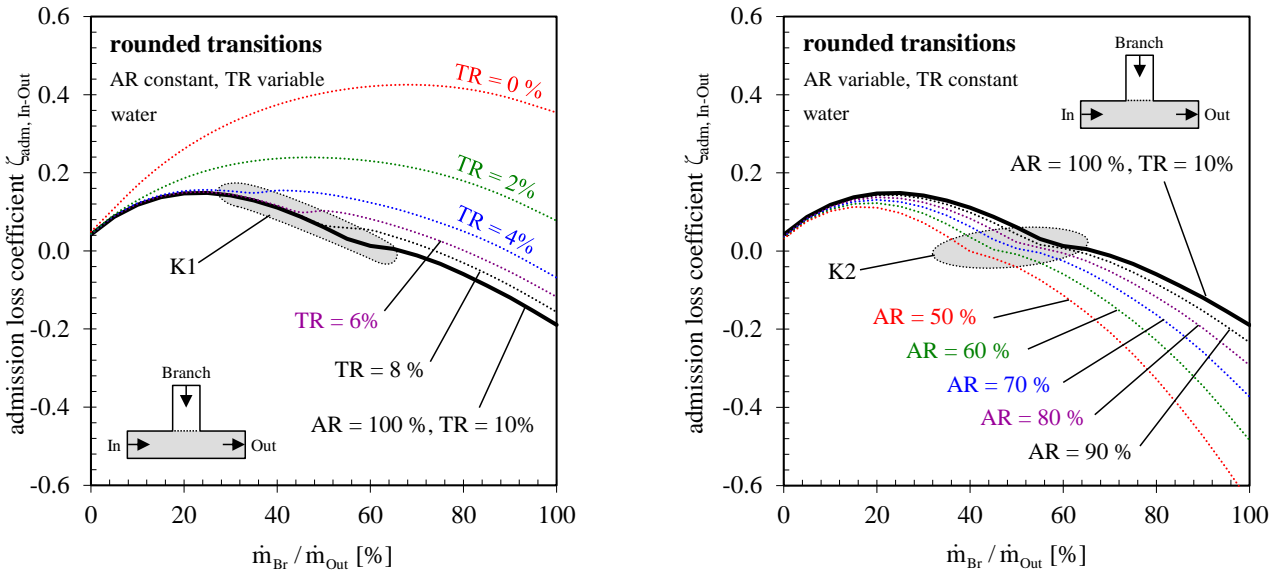


Figure 7: Geometrical influence on the admission loss coefficient $\zeta_{adm, In-Out}$ for the T-junction with rounded transitions; left: variation of TR; right: variation of AR

As depicted in the left diagram of Figure 7, the admission loss $\zeta_{adm, In-Out}$ is increased with a reduction of the transition radius TR. Engelmann et al. (2014) reported that this characteristic is associated with an earlier separation of the deflected flow from the wall (highlighted as kink K1 in the diagram) together with a longer axial spread of the separation zone. Against that, the right diagram of Figure 7 shows a contrary behaviour. When the area ratio AR is reduced the separation point of the deflected branch flow moves to smaller flow ratios (see kink K2) because of the higher branch momentum whereas the overall loss curve is decreased. Combining both geometrical parameters leads to a compensation of the loss spread (see Figure 6, left) and therefore to the small $\Delta\zeta_{adm, In-Out}$.

It is a little bit different for $\zeta_{adm, Br-Out}$ as Figure 8 shows. A reduction of the transition radius TR leads to an increase of the loss distribution equally to Figure 7. However, reducing the area ratio AR results in an increase of the admission loss coefficient, which is opposed to Figure 7. The separation of the deflected flow is still present in the loss distribution in Figure 8 but not clearly recognizable because of the higher admission loss magnitude compared to Figure 7. Again, combination of both effects leads to the wide spread $\Delta\zeta_{adm, Br-Out}$ in Figure 6 (right diagram). Although loss values of numerical results and literature data differ because of the missing sidewalls effect they show the same characteristic loss distribution. Moreover, it is an interesting issue that the kinks K1 to K4 are not considered in the literature in any way.

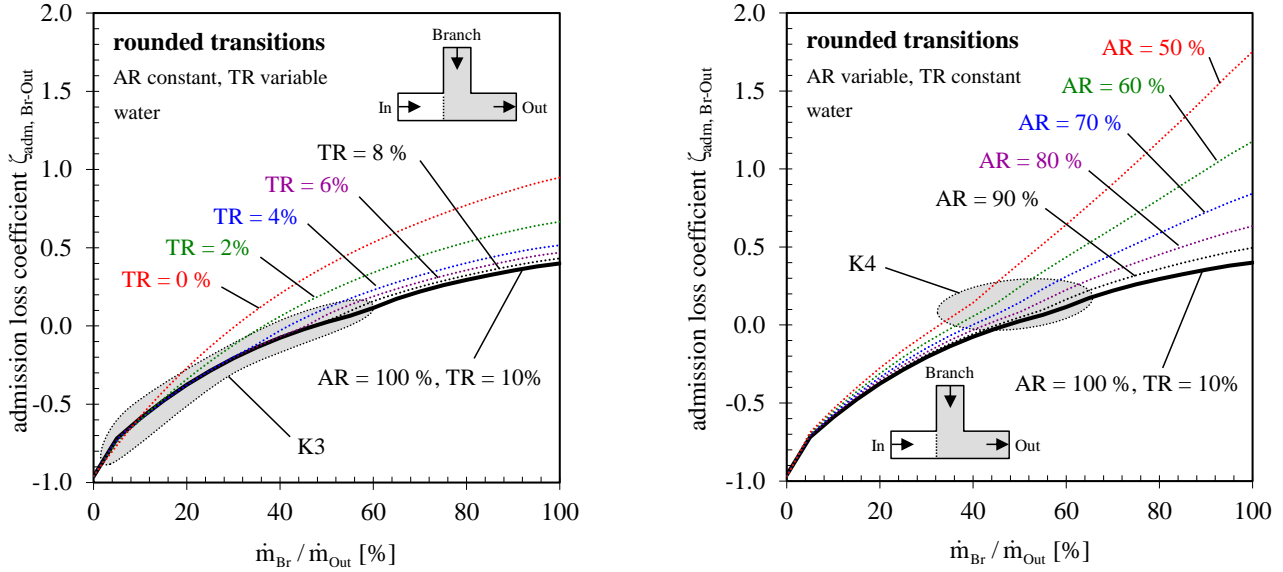


Figure 8: Geometrical influence on the admission loss coefficient $\zeta_{adm, Br-Out}$ for the T-junction with rounded transitions; left: variation of TR; right: variation of AR

Influence of the temperature level on the loss distribution

Following the illustration of geometrical influences, this passage shows how the temperature level affects the admission loss for flow junctions which, unfortunately, is not described in the literature. As depicted in Figure 9, there are two parameters which are influencing the loss distribution: on the one hand the overall temperature level of the computational domain represented by the inlet total temperature $T_{t,In}$ and on the other hand the branch total temperature $T_{t,Br}$.

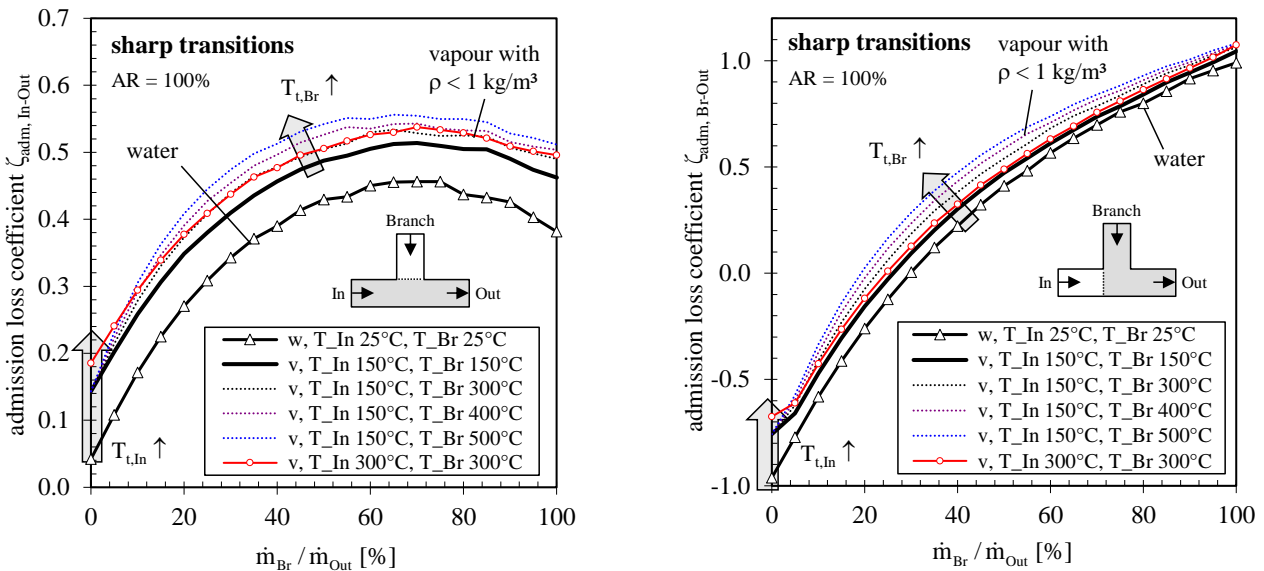


Figure 9: Influence of the temperature level on the admission loss coefficient $\zeta_{adm, In-Out}$ and $\zeta_{adm, Br-Out}$ for the T-junction with sharp transitions, AR = 100%

As given in the diagrams in Figure 9 and highlighted with arrows, increasing $T_{t,Br}$ results in higher loss values for intermediate and high flow ratios whereas the overall loss level is raised by $T_{t,In}$ (see curves with dots for vapour at 300° C). This behaviour is attributable to the density of the vapour if the specific equation for ideal gas is considered. Increasing the temperature level and keeping the pressure level constant at once lead to a reduction of the density. Involving the

continuity equation for a specific and therefore constant mass flow ratio FR shows that a reduction of the density leads to a higher channel respectively pipe velocity. This means a higher flow momentum is present together with higher shear forces within the fluid. But no matter which temperature is chosen the loss curve for water as incompressible fluid is always located beneath the corresponding curves for vapour.

Influence of the pressure level on the loss distribution

The pressure level affects the admission loss in the same way as the temperature level does. Thus, resulting admission loss curves for predictions with several total pressure levels are drawn in the diagrams of Figure 10. Please note: the total temperature of the numerical domain is raised from a base value of 150° C up to of 300° C for all corresponding simulations. This is necessary to avoid a condensation of the overheated steam at 2, 5 and 10 bar. The new base loss curve is plotted with dots and for comparison already used in Figure 9.

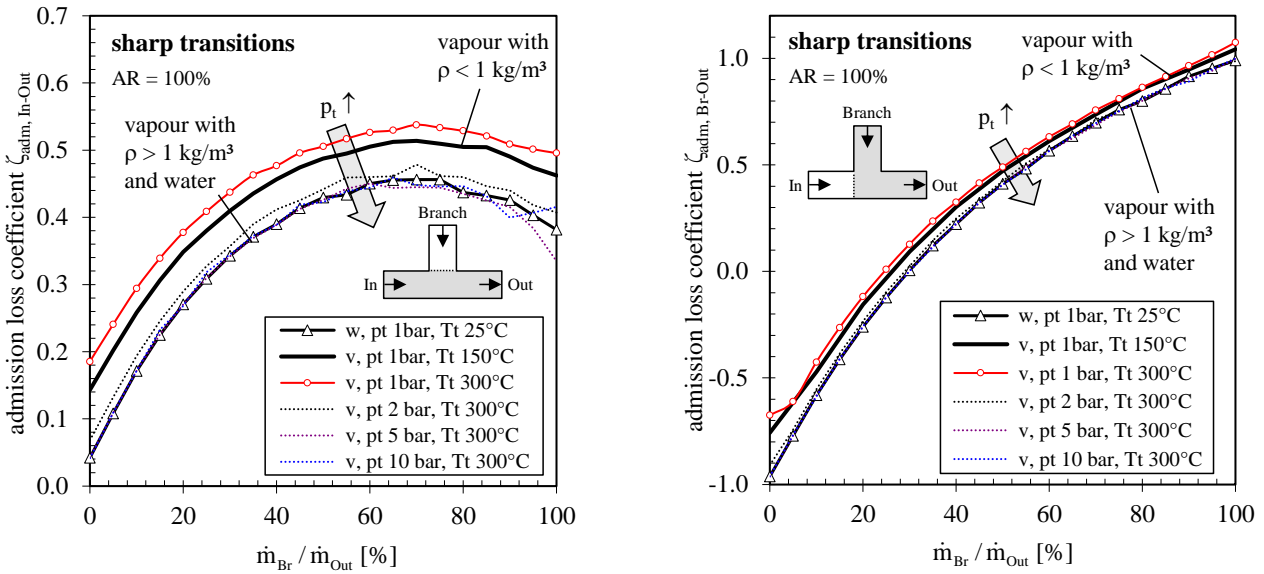


Figure 10: Influence of the pressure level on the admission loss coefficient $\zeta_{adm, In-Out}$ and $\zeta_{adm, Br-Out}$ for the T-junction with sharp transitions, AR = 100%

The arrows in Figure 10 indicate that a higher pressure level leads to a reduction of the admission loss. This behaviour again is provoked by density shifts in combination with the ideal gas equation. An increase of the pressure level leads to an increase of the density and therefore reduces the channel velocity together with corresponding loss inducing effects. As indicated in Figure 9 and Figure 10, a density of 1 kg/m³ can be seen as limiting value. Values above reduce the admission loss coefficient while values below increase it.

Variation of the pressure ratio and its effect on the admission loss

In prior publications and also in the graphs above all loss curves are generated and drawn as a function of the flow ratio. But another path is taken in this study. That means in detail not the mass flow but the total pressure is set as boundary condition at inlet of main and branch channel for the numerical predictions. The total pressure at the inlet is set to 2 bar whereas the total temperature of the numerical domain amounts to 300° C. Additionally, the branch total pressure is gradually increased starting with a total pressure ratio $p_{t,Br} / p_{t,In}$ of 0.95 up to a maximum of 1.25. The corresponding mass flow ratios are calculated during the simulations as function of the actual total pressure ratio. The resulting admission loss curves for several area ratios are given in Figure 11 whereas specific flow ratios FR using a step size of 25% are highlighted with symbols.

As both diagrams in Figure 11 show: the smaller the area ratio AR the larger the reachable total pressure ratio. This effect can be explained with the conservation of momentum. For a constant momentum at the branch inlet that means at a given specific velocity and mass flow the pressure depends solely on the area ratio which are inversely proportional to each other. Furthermore, the distribution of the associated flow ratio curves mirrors that $\zeta_{adm, In-Out}$ is nearly independent from the area ratio for sharp transitions (reported by Engelmann et al. (2013)) and rounded transitions (see Figure 6, left) as opposed to $\zeta_{adm, Br-Out}$ (compare Figure 6, right). Another point becomes obvious if the scales of the two diagrams are compared with each other. The maximum for $\zeta_{adm, Br-Out}$ reaches nearly sevenfold of the $\zeta_{adm, In-Out}$ which is important if one wants to consider the admission loss for the branch channel.

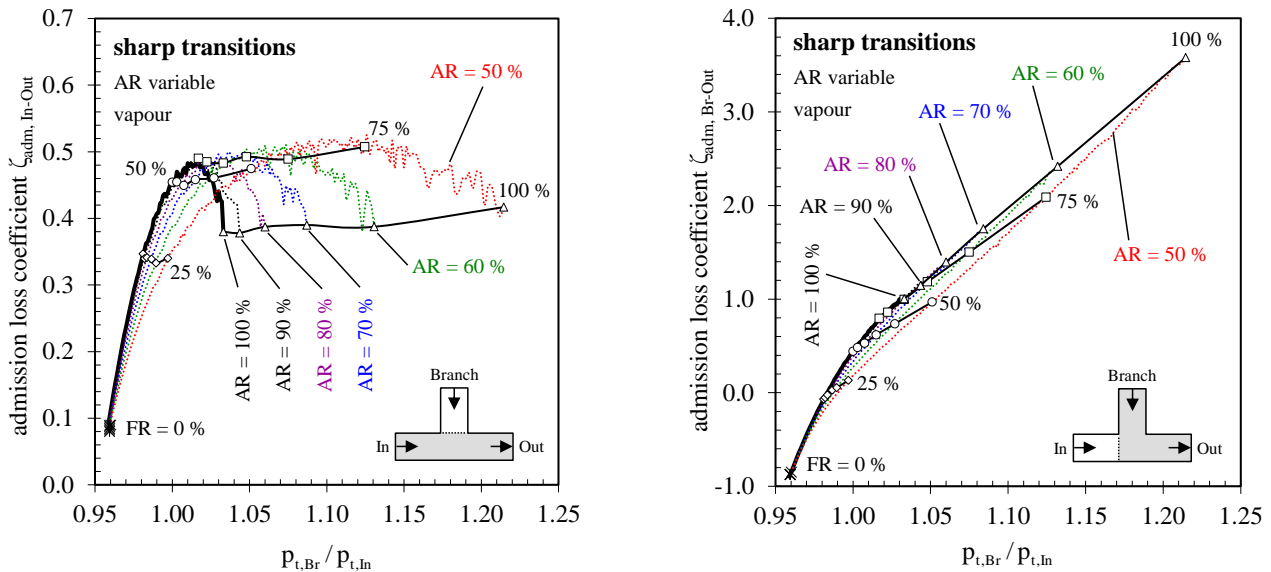


Figure 11: Variation of the branch total pressure and its influence on the admission loss coefficient $\zeta_{adm, In-Out}$ and $\zeta_{adm, Br-Out}$ for the T-junction with sharp transitions

All results which are described above are obtained for T-junctions with sharp transitions. Although junctions with rounded transitions produce lower admission losses (compare Figure 4 with Figure 5) the main characteristics based on pressure and temperature influence are adaptable.

CONCLUSIONS

This paper deals with the loss generation process caused by steam admission in a generic T-junction with a detailed view on several parameters such as geometry, temperature and pressure. The first part describes the parametric model of the T-junction which is used for the numerical predictions as well as illustrates the loss calculation method to gain the amount of total pressure, friction and admission loss. The numerical results for both accounting methods (inlet to outlet and branch to outlet) are presented in the second part. Two fluids are used for the predictions. Water is used for validation with literature data while vapour is applied to ensure transferability to steam turbines. Although a good agreement with the literature is gained some characteristic deviations caused by geometrical differences of pipe- and T-junction exist, e.g. the appearance of kinks in the specific loss curves evoked by a separation of the deflected flow coming from the branch.

Furthermore, a variation of the temperature and pressure level shows a significant shift of the admission loss distribution which in both cases is a function of compressibility and therefore of the density. The total pressure ratio at branch and inlet affects the admission loss, too. As the results show a small area ratio expands the reachable pressure ratio which is attributed to the conservation of momentum.

Unfortunately, in literature admission loss information for compressible fluids are not provided to date. Thus, it is recommended to build up a test rig including the described generic junction in order to gather appropriate validation data and to prove the characteristic flow effects. Further numerical work will deal with the influences of inflow angle variations, a mixed accounting considering inlet, branch and outlet at the same time as well as with more predictions of steam turbine sections.

REFERENCES

Andersson, U., Westin, J., Eriksson, J., 2006. Thermal Mixing in a T-junction. Tech. Rep. U 06-66, Vattenfall Research and Development AB.

Barringer, M., Thole, K. A., Krishan, V. and Landrum, E. (2014), "Manufacturing Influences On Pressure Losses of Channel Fed Holes", Trans. ASME, Journal of Turbomachinery", Vol. 136, pp 051012-1-10.

Denton, J. (1993), "Loss Mechanisms in Turbomachines", Trans. ASME, Journal of Turbomachinery, Vol. 115, pp 21-656.

Engelmann, D., Schramm, A., Polklas, T. and Mailach, R., (2014), "Losses of Steam Admission in Industrial Steam Turbines Depending on Geometrical Parameters", ASME Turbo Expo, Paper-No. GT2014-25172.

Engelmann, D., Schramm, A., Polklas, T., Schwarz, M., A. & Mailach, R. (2013), "Enhanced Loss Prediction for Admission through Circumferential Slots in Axial Steam Turbines", Conference Proceedings of the 10th European Conference on Turbomachinery, pp 350-359.

Engelmann, D., Kalkkuhl, T. J., Polklas, T. and Mailach, R. (2012), "Influence of Shroud Cavity Jet and Steam Admission through a Circumferential Slot on the Flow Field in a Steam Turbine", ASME Turbo Expo, Paper-No. GT2012-68465.

Gier, J., Stubert, B., Brouillet, B. and de Vito, L. (2003), "Interaction of Shroud Leakage Flow and Main Flow in a Three-Stage LP Turbine", ASME Turbo Expo, Paper-No. GT2003-38025.

Idelchik, I. E. (1986): "Handbook of Hydraulic Resistance (2nd Edition)", Hemisphere Publishes, Diagrams 7-4 & 7-11.

Kuczaj, A. K., Komen, E.M.J. and Loginov, M.S. (2010) "Large-Eddy Simulation study of turbulent mixing in a T-junction", Nuclear Engineering and Design, Vol. 240, pp 2116–2122.

Miller, D. S. (1990): "Internal Flow Systems (2nd Edition)", British Hydromechanics Research Association, Figures 13.10, 13.11, 13.14 & 13.15.

Schlichting, H. and Gersten, K. (2006), „Grenzschicht-Theorie“, 10th Edition, Springer, Berlin.

Walker, C., Manera, A., Niceno, B., Simiano, M. and Prasser, H.-M. (2010), "Steady-state RANS-simulations of the mixing in a T-junction", Nuclear Engineering and Design, Vol. 240, pp 2107-2115.

Wallis, A. M., Denton, J. D. and Demarge, A. A. J. (2000), "The Control of Shroud Leakage Flows to Reduce Aerodynamic Losses in a Low Aspect Ratio Shrouded Axial Flow Turbine", ASME Turbo Expo, Paper-No. 2000-GT-475.